

RESEARCH ARTICLE

The N-terminal p.(Ser38Cys) *TIMP3* mutation underlying Sorsby fundus dystrophy is a founder mutation disrupting an intramolecular disulfide bond

Sarah Naessens¹  | Julie De Zaeytijd²  | Delfien Syx¹  |
 Roosmarijn E. Vandenbroucke^{3,4}  | Frédéric Smeets²  | Caroline Van
 Cauwenbergh^{1,2}  | Bart P. Leroy^{1,2,5}  | Frank Peelman^{6,7}  | Frauke Coppieters¹ 

¹Center for Medical Genetics Ghent, Ghent University and Ghent University Hospital, Ghent, Belgium

²Department of Ophthalmology, Ghent University Hospital, Ghent, Belgium

³VIB Center for Inflammation Research, VIB, Ghent, Belgium

⁴Department of Biomedical Molecular Biology, Ghent University, Ghent, Belgium

⁵Division of Ophthalmology, The Children's Hospital of Philadelphia, Philadelphia, Pennsylvania, USA

⁶Receptor Research Laboratories, Cytokine Receptor Lab, VIB-UGent Center for Medical Biotechnology, Ghent, Belgium

⁷Department of Biochemistry, Ghent University, Ghent, Belgium

Correspondence

Frauke Coppieters, Center for Medical Genetics Ghent, Ghent University and Ghent University Hospital, Corneel Heymanslaan 10, 9000 Ghent, Belgium.

Email: frauke.coppieters@ugent.be

Funding information

Fund for Scientific Research (FWO), Flanders, Belgium (1S60616N, 12D8715N, 1515615N, 12Q5917N).

Communicated by Daniel F. Schorderet

Abstract

Sorsby fundus dystrophy (SFD) is a macular degeneration caused by mutations in *TIMP3*, the majority of which introduce a novel cysteine. However, the exact molecular mechanisms underlying SFD remain unknown. We aimed to provide novel insights into the functional consequences of a distinct N-terminal mutation. Haplotype reconstruction in three SFD families revealed that the identified c.113C>G, p.(Ser38Cys) mutation is a founder in Belgian and northern French families with a late-onset SFD phenotype. Functional consequences of the p.(Ser38Cys) mutation were investigated by high-resolution Western blot analysis of wild type and mutant *TIMP3* using patient fibroblasts and *in vitro* generated proteins, and by molecular modeling of *TIMP3* and its interaction partners. We could not confirm a previous hypothesis on dimerization of mutant *TIMP3* proteins. However, we identified aberrant intramolecular disulfide bonding. Our data provide evidence for disruption of the established Cys36-Cys143 disulfide bond and formation of a novel Cys36-Cys38 bond, possibly associated with increased glycosylation of the protein. In conclusion, we propose a novel pathogenetic mechanism underlying the p.(Ser38Cys) *TIMP3* founder mutation involving intramolecular disulfide bonding. These results provide new insights into the pathogenesis of SFD and other retinopathies linked to mutations in *TIMP3*, such as age-related macular degeneration.

KEYWORDS

aberrant disulfide bonding, dimerization, founder mutation, glycosylation, Sorsby fundus dystrophy, *TIMP3*

1 | INTRODUCTION

Sorsby fundus dystrophy (SFD; MIM# 136900) is a rare, autosomal dominant retinal dystrophy in which patients experience a sudden loss of central vision related to the development of choroidal neovascularization (CNV) or macular atrophy during the fourth or fifth decade of life (Sorsby, Joll Mason, & Gardener, 1949). The disease is characterized by thickening of the Bruch membrane, chorioretinal atrophy, and multiple drusen-like deposits throughout the entire fundus.

These deposits are very similar to findings in early age-related macular degeneration (AMD; MIM# 603075) (Gourier & Chong, 2015), however the diffuse Bruch membrane thickening observed in SFD is not limited to the macula as in AMD. Typical manifestations include night blindness, scotoma, and metamorphopsia with subsequent reduced central, detailed vision and color vision problems (Christensen, Brown, Cree, Ratnayaka, & Lotery, 2017). In the more advanced stages, peripheral vision is lost with the development of widespread atrophy, with any remaining function hampered by periph-

This is an open access article under the terms of the Creative Commons Attribution-NonCommercial-NoDerivs License, which permits use and distribution in any medium, provided the original work is properly cited, the use is non-commercial and no modifications or adaptations are made.

© 2019 The Authors. *Human Mutation* published by Wiley Periodicals, Inc.

eral CNV and scarring (Felbor et al., 1997; Gliem et al., 2015). Management of CNV in the later stages of the disease can be successful using vascular endothelial growth factor (VEGF)-inhibitors (Gourier & Chong, 2015). SFD is a fully penetrant disease with large interfamilial and intrafamilial variability in age of onset, progression rate, and morphological features (Christensen et al., 2017; Gliem et al., 2015).

SFD is caused by mutations in *TIMP3* (MIM# 188826), which is a member of the family of tissue inhibitor of matrix metalloproteinases (TIMPs). TIMPs are key regulators of the matrix metalloproteinases (MMPs), zinc-dependent endopeptidases that degrade the extracellular matrix (ECM) and shed cell surface molecules (Brew & Nagase, 2010; Clark, Swingler, Sampieri, & Edwards, 2008). *TIMP3* is unique among its family members as it is the only TIMP localized to the ECM (Qi & Anand-Apte, 2015; Visse & Nagase, 2003). The protein is secreted by the retinal pigment epithelium (RPE) and deposited in the ECM of the Bruch membrane, where it regulates the thickness of the Bruch membrane by inhibiting MMPs (Weber, Vogt, Pruetz, Stöhr, & Felbor, 1994). Mutations in *TIMP3* result in an increased accumulation of the *TIMP3* protein and a thickening of Bruch membrane, leading to reduced permeability for trafficking metabolites and nutrients (Kamei & Hollyfield, 1999). However, the exact molecular mechanisms underlying SFD remain unknown.

Each TIMP contains an N- and C-terminal domain, which fold into a highly conserved tertiary structure. The N-terminal domain forms a ridge that fits into the active site of the MMPs, thus inhibiting these MMPs (Li, Clarke, Barker, & McKie, 2005; Nagase, Visse, & Murphy, 2006), whereas the C-terminal domain ascertains the interaction with the ECM and inhibits activation of pro-MMPs (Brew & Nagase, 2010; Nagase et al., 2006). The three-lobed structure of each domain is maintained by three disulfide bonds, formed by 12 conserved cysteine residues in total (Li et al., 2005; Nagase et al., 2006). To date, 18 distinct mutations causing SFD have been identified (Christensen et al., 2017), the majority of which are missense mutations located in the C-terminal domain of the protein (Bakall, Sohn, Riley, Brack, & Stone, 2014; Schoenberger & Agarwal, 2013). One mutation causes the loss of a cysteine, whereas 13 mutations result in an additional cysteine residue (Gliem et al., 2015). Most studies hypothesize that mutant *TIMP3* proteins with unpaired cysteines form abnormal disulfide-bonded dimers and aggregates that decrease the turnover of the protein in the Bruch membrane, thus leading to a disturbed homeostasis in ECM remodeling and thickening of Bruch membrane (Arris et al., 2003; Langton, Barker, & McKie, 1998; Langton, McKie, Smith, Brown, & Barker, 2005; Langton et al., 2000; Lin, Blumenkranz, Binkley, Wu, & Vollrath, 2006; Saihan et al., 2009; Soboleva, Geis, Schrewe, & Weber, 2003; Weber et al., 2002; Yeow et al., 2002). Despite this widely accepted hypothesis, no study already proved the existence of novel disulfide bonds, either intra- or intermolecular. Importantly, abnormal disulfide bonding cannot be the only cause of SFD as two missense mutations do not lead to the introduction or loss of a cysteine. Controversy also exists about the dimerization capacity of the p.(Ser179Cys) *TIMP3* mutant, as some show dimerization of the mutant (Langton et al., 2005) and others not (Qi et al., 2002). Overall, these findings underscore our current lack in understanding the pathogenetic mechanism underlying SFD.

In 2000, Assink et al. examined a large Belgian family with typical SFD. Although linkage was found with the 22q12.1-q13.2 region containing *TIMP3*, no *TIMP3* mutation was identified (Assink et al., 2000). Here, it was our aim to elucidate the genetic cause of SFD in this family and two other SFD families, and functionally characterize the mutant proteins.

2 | MATERIALS AND METHODS

2.1 | Editorial policies and ethical considerations

Research protocols adhered to the tenets of the Declaration of Helsinki and were approved by the ethical committee of Ghent University (B670201733128). Patients provided written informed consent for the study.

2.2 | Clinical evaluation of patients

Three seemingly unrelated families diagnosed with SFD, two Belgian and one French, were investigated. A detailed ophthalmologic examination at baseline (consultation at presentation) included assessment of Snellen best-corrected visual acuity (BCVA) and refraction, slit-lamp examination, Goldmann applanation tonometry, dilated ophthalmoscopy and extensive fundus imaging using standard color fundus photography (Topcon TRC-50EX fundus camera; Topcon Corporation, Tokyo, Japan), confocal scanning laser ophthalmoscopy with blue and near-infrared auto-fluorescence (BAF and NIR-AF), near-infrared reflectance (NIR-R) and red-free (RF) imaging (cSLO; Heidelberg Retina Angiograph HRA2; Heidelberg Engineering, Dossenheim, Germany), and spectral domain optical coherence tomography (SD-OCT, Heidelberg Spectralis OCT; Heidelberg Engineering, Dossenheim, Germany). Existing clinical records were revisited and a full medical history was obtained to provide detailed clinical data for each patient. Patients were investigated and questioned about age and mode of onset and the natural course of the disease over the years.

Eighteen individuals of family 1 underwent ophthalmological examination (Figure 1a). Family 2 consists of four individuals: two siblings and their parents (Figure 1b). Family 3 consists of only the index patient (Figure 1c).

2.3 | Mutation analysis of *TIMP3*

All five *TIMP3* (RefSeq NM_000362.4) coding exons and adjacent splice sites were amplified from genomic DNA by polymerase chain reaction (PCR) (Supporting Information Table S1). PCR products underwent Sanger sequencing using the BigDye[®] Terminator Cycle Sequencing kit on an ABI3730xl DNA analyzer (both Applied Biosystems). The obtained sequences were analyzed with the SeqScape software (Applied Biosystems). All genomic positions are based on genome build GRCh37/hg19.

2.4 | Haplotyping of the *TIMP3* p.(Ser38Cys) mutation

The haplotype was determined based on five probands from family 1 (IV:31, IV:56, IV:59, V:30, and V:33), two siblings from family 2 (II:1

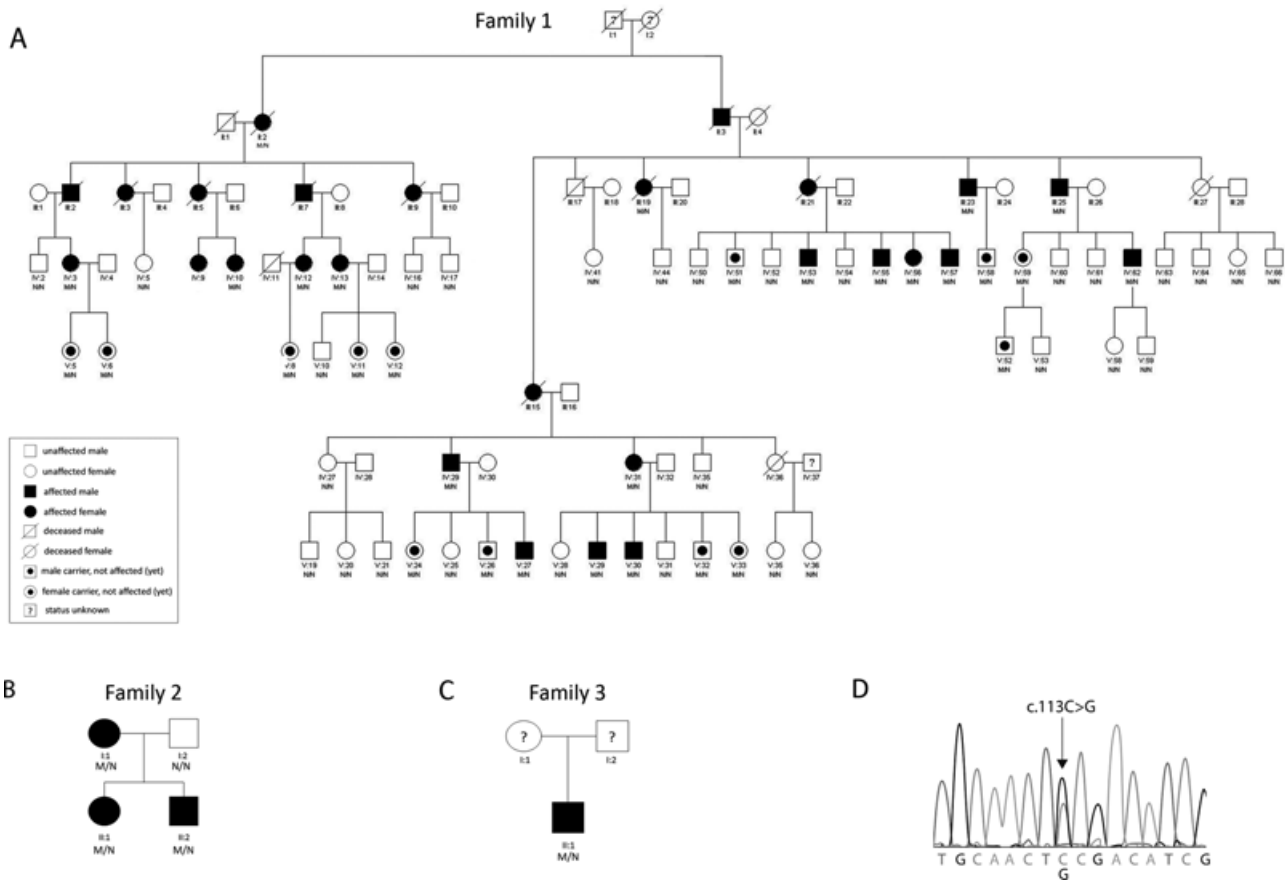


FIGURE 1 Pedigrees of families segregating the *TIMP3* c.113C>G mutation. (a) Reduced pedigree of family 1. Only the branches for which segregation analysis was done are shown. (b) Pedigree of family 2. For family 1 and 2, co-segregation of the mutation was shown with disease. (c) Pedigree of family 3. For family 3, no individuals were available for segregation analysis. (d) Sequence electropherogram of the heterozygous c.113C>G, p.(Ser38Cys) (RefSeq NM_000362.4) variant. Abbreviations used: M = mutant allele, N = normal allele

and II:2), and one proband from family 3 (II:1) (Figure 1a–c). Haplotyping was performed using 35 single nucleotide polymorphisms (SNPs), covering a 9 Mb region surrounding the *TIMP3* gene. The genotype of each SNP was analyzed with PCR and Sanger sequencing. Primer sequences and SNP details are listed in Supporting Information Tables S1 and S2.

2.5 | *TIMP3* expression analysis

Dermal fibroblasts derived from a skin biopsy of two patients (IV:56 and IV:59) of family 1 and four age-matched control individuals were cultured in Dulbecco's minimal essential medium (MEM) with phenol red (Thermo Fisher Scientific, 41966) supplemented with 10% fetal calf serum, 1% penicillin-streptomycin, and 1% MEM nonessential amino acids. Cells were seeded in six well plates in triplicate at 300,000 cells per well and grown for 48 hr until confluence. Total RNA was extracted by scraping the wells and RNA extraction was done using the RNeasy® mini kit (Qiagen) with on-column DNase digestion (Qiagen) according to manufacturer's instructions. A second DNase treatment was done using the Heat&Run gDNA removal kit (ArcticZymes) according to manufacturer's instructions. cDNA was synthesized with the iScript cDNA synthesis kit (Bio-Rad Laboratories) using 500 ng of mRNA, followed by reverse-transcription quantitative PCR (RT-qPCR) using SsoAdvanced Universal SYBR Green Supermix (Bio-Rad Labora-

tories). The expression level of *TIMP3* was determined using intron-spanning primers (primerXL (Lefever et al., 2017)). Data analysis was done using the qBase+ software (Biogazelle) with following reference genes for normalization: *HMBS*, *YWHAZ*, and *SDHA*. Primer sequences are listed in Supporting Information Table S1.

2.6 | Preparation of fibroblast cells and Western blot analysis

Dermal fibroblast cultures of two patients (IV:56 and IV:59) and age-matched controls were cultured as described above. Cells were seeded at 300,000 cells per well in six well plates and were grown until confluence. After 48 hr, transforming growth factor beta-1 (TGFβ1, 20 μg·ml⁻¹) was added 24 hr prior to cell lysis to stimulate *TIMP3* expression. Cell lysates were collected by scraping the cells in Laemmli lysis buffer or M-PER mammalian protein extraction reagent (Thermo Scientific) complemented with complete protease inhibitor cocktail (Sigma-Aldrich) and phosphatase inhibitors (Sigma-Aldrich). Protein concentrations were measured using the Pierce BCA protein assay kit (Thermo Scientific). Equal amounts (30 μg) of protein sample were reduced by incubation at 98°C with 1 M DTT and subjected to SDS-PAGE using NuPAGE™ 4–12% Bis-Tris protein gels (Invitrogen, Life Technologies). Subsequently, proteins were transferred to a nitrocellulose membrane using the iBlot® 2 System (Life Technologies).

In general, Western blots were first optimized using two different membrane blocking buffers (2% membrane blocking agent (GE Healthcare Life Sciences)) in 1x Tris-buffered saline with Tween-20 (TBST) or 2% BSA in TBST and different antibody concentrations, ranging between 1:500 and 1:2000.

Membranes were incubated in blocking buffer (TBST, 2% membrane blocking agent (GE Healthcare Life Sciences)) for 2 hr at room temperature and immunolabeled with primary antibody (T7687, Sigma-Aldrich or MAB3318, Calbiochem) diluted 1:1000 in blocking buffer for 16 hr at 4°C. Membranes were probed with secondary antibody (anti-rabbit IgG and anti-mouse IgG, HRP-linked antibody (Cell Signaling Technologies)) diluted 1:2500 in blocking buffer for 2 hr at room temperature. Membranes were developed using the SuperSignal® West Dura Extended Duration Substrate kit (Thermo Scientific, Life Technologies) and scanned with the ChemiDoc-It® 500 Imaging System (UVP).

In blots with M-PER cell lysates, relative densities of glycosylated TIMP3 were calculated on three independent Western blots using Image J. Relative ratios of glycosylated TIMP3 were calculated to the total amount of TIMP3 present in the sample. Statistical analysis was done using an unpaired *t*-test. Furthermore, β -tubulin was used as internal loading control. For this, membranes were stripped using the Restore PLUS Western Blot Stripping Buffer (Life Technologies) and probed with β -tubulin primary antibody (ab6046, Abcam) diluted 1:2000 in blocking buffer for 1 hr at room temperature and subsequently probed with secondary antibody (anti-rabbit IgG, HRP-linked antibody (Cell Signaling Technologies)) diluted 1:2500 in blocking buffer for 1 hr at room temperature. Developing was done as described above.

ECM extracts were made by removing dermal fibroblasts from the well by trypsinization, subsequent washing with phosphate buffered saline (PBS) and scraping of the remaining proteins in ECM buffer containing 100 mM Tris-HCl [pH 6.8], 10% glycerin, and 1% SDS (Weber et al., 2002). SDS-PAGE and protein transfer to nitrocellulose membrane was performed as described above. Membranes were blocked for 2 hr and immunolabeled with primary antibody (AB6000, Merck Millipore, 1:2000 or MAB3318, Calbiochem, 1:1000), respectively diluted in 2% BSA or 2% membrane blocking agent in TBST for 16 hr at 4°C. Membranes were probed with secondary antibody and developed as described above.

2.7 | *In vitro* transcription and translation of TIMP3 protein and subsequent Western blot analysis

We constructed wild type (WT) and mutant (c.113C>G, p.(Ser38Cys) and c.536C>G, p.(Ser179Cys)) expression constructs starting from the Gateway pcDNA-DEST47 vector (Invitrogen, Life Technologies) and a WT or mutant TIMP3 open reading frame (ORF) containing vector (Integrated DNA Technologies) using a combined Gateway BP-LR-recombination reaction (Invitrogen, Life Technologies). Plasmids were transformed in One Shot TOP10 competent cells (Invitrogen, Life Technologies) and subsequently isolated with the NucleoBond Xtra Midi/Maxi kit (Macherey-Nagel). The entire TIMP3 inserts and the surrounding backbone were Sanger sequenced and selected plasmids were grown to obtain larger quantities.

In vitro transcription and translation of generated WT and mutant expression constructs was done using the T7 TnT® Quick Coupled Transcription/Translation System (Promega) according to manufacturer's instructions. Briefly, 1 μ g of expression construct was incubated for 75 min at 30°C together with 40 μ l of TNT Quick Master mix, 1 μ l Methionine, and 1 μ l PCR enhancer. Generated proteins were treated with RNase A (0.2 μ g· μ l⁻¹) for 5 min at 30°C. Protein concentration was determined using the Pierce BCA protein assay kit (Thermo Scientific) and equal amounts of protein (30 μ g) were subjected to SDS-PAGE on NuPAGE™ 4–12% Bis-Tris Protein Gels or Novex™ 10–20% Tris-Glycine protein gels (Invitrogen, Life Technologies). Anti-TIMP3 antibodies (AB6000, Merck Millipore, 1:2000 or MAB3318, Calbiochem, 1:1000) were used as described earlier.

2.8 | Molecular modeling of TIMP3–MMP2 interaction

A homology model for full-length TIMP3 was generated using the homology modeling command in YASARA structure (version 17.8.15) using the structure of TIMP2 (PDB code: 1GXD, chain D) as a template (<http://yasara.org/products.htm#structure>). Homology modeling used a MAFFT alignment (Supporting Information Figure S1A) guided by structural alignment of TIMP2 (1GXD) and the TIMP3 N-terminal domain (3CKI) (Katoh & Standley, 2013). A model for the complex of full-length TIMP3 with pro-MMP2 was generated as above, but now using TIMP2 and pro-MMP2 as templates, as present in the 1GXD template structure (chain A and C). A model of TIMP3 with MMP2 was generated by superposing the structure of the MMP2 protease domain (PDB code: 1QIB) on the TACE protease domain in the TIMP3/TACE crystal structure (PDB code: 3CKI) using UCSF chimera matchmaker, superposing only a selection of residues around the metal binding site (Supporting Information Figure S1B) (Pettersen et al., 2004). After removal of the TACE structure, residues 100–121 of TIMP3 were replaced by residues of the full-length TIMP3 homology model using YASARA structure, generating a model of full-length TIMP3 with MMP2. The model was energy minimized using the YASARA em_runclean macro.

The effect of mutations on protein structure was analyzed using the YASARA structure md_refine protocol, which combines 500 ps molecular dynamics, with energy minimization of frames taken at 25 ps intervals. The mutation was tested in the crystal structure of the TIMP3 N-terminal domain (PDB code: 3CKI, without TACE) and in the homology model of full-length TIMP3. Both WT and mutant were subjected to five different md_refine runs. The energy minimized structures with lowest energy of each simulation, and the structures after 400, 425, 450, 475, and 500 ps simulation were all compared after different structural superpositions in UCSF chimera and YASARA. Visual inspection of the superpositions revealed no reproducible visible differences between the WT and mutant models.

2.9 | Prediction of the effect of the p.(Ser38Cys) mutation on protein stability

The effect of the p.(Ser38Cys) mutation on the protein stability was tested using FoldX (Guerois, Nielsen, & Serrano, 2002), DUET

(Pires, Ascher, & Blundell, 2014), and MAESTRO (Laimer, Hofer, Fritz, Wegenkittl, & Lackner, 2015). FoldX calculations used the FoldX Build-Model protocol after RepairPDB preparation of the structure or model. DUET calculations used the DUET webserver (<http://biosig.unimelb.edu.au/duet/stability>), and generated DUET, MCSm, and DSM stability scores. MAESTRO calculations used the MAESTROweb web-server (<https://biwww.che.sbg.ac.at/maestro/web>).

2.10 | Generation of mutant (p.(Cys36Ser) and p.(Cys143Ser)) constructs and *in vitro* transcription and translation

The c.107G>C, p.(Cys36Ser) and c.428G>C, p.(Cys143Ser) mutations were inserted into WT or mutant (c.113C>G, p.(Ser38Cys)) *TIMP3* expression constructs, used to predict the effect of the p.(Ser38Cys) mutation on disulfide bond formation. The mutations were inserted using the Q5 site-directed mutagenesis kit (New England Biolabs), and mutation-specific primers were designed with the NEBaseChanger software (New England Biolabs) (Supporting Information Table S1). Mutated plasmids were transformed in One Shot TOP10 competent cells (Invitrogen, Life Technologies) and subsequently isolated with the NucleoBond Xtra Midi/Maxi kit (Macherey-Nagel). The entire *TIMP3* insert was sequenced and selected plasmids were grown to obtain larger quantities. Sequencing primers can be found in Supporting Information Table S1. *In vitro* transcription and translation was performed as described above.

3 | RESULTS

3.1 | Clinical evaluation of three SFD families

Supporting Information Table S3 summarizes the phenotypic data for the three families. Only one third of the patients explicitly complained about night blindness in their fifth decade. The other patients did not, although the majority of them were older than 50 years. In one patient photophobia was more important early on in the disease course.

When examined in the third decade, the fundus appearance was considered to be normal or near-normal with only few small white deposits with limited RPE alterations. Patients in their fourth decade often showed fine drusen located in the mid-periphery beyond the temporal vascular arcades without obvious or important macular changes. This evolved toward a 360° spread of numerous drusen in the mid-periphery in the fifth decade with both RPE pigmentary changes in the far periphery and early macular changes. Further on, CNV develops together with fibrosis and RPE hyperplasia and atrophy not only confined to the posterior pole but also present in the (mid-) periphery. All patients kept an optimal best-corrected visual acuity in at least one eye until the sixth decade (with the exemption of one patient). Patients in the seventh decade or older had rapidly evolved toward legal blindness due to macular scarring and/or atrophy. However, in these older patients CNVs commenced unfortunately in a pre-anti-VEGF era and therefore rapid scarring was unavoidable (Figure 2). Two patients continue to undergo regular intravitreal injections with anti-VEGF (off-

label bevacizumab). In one patient, this was advised despite BCVA loss and macular scarring in order to reduce peripheral CNV activity and to preserve peripheral visual function.

None of our patients had pulmonary involvement. Although, currently, no further investigations were performed to detect asymptomatic air trapping in the absence of clinical signs, symptoms, or complaints.

3.2 | Identification of a p.(Ser38Cys) mutation in the *TIMP3* gene in three SFD families

We performed Sanger sequencing of all five coding exons and surrounding exon-intron borders of *TIMP3*. This revealed a mutation in the first exon of family 1: c.113C>G, p.(Ser38Cys) (NM_000362.4) (Figure 1d). This is a known pathogenic variant in the *TIMP3* gene and one of only two mutations currently identified in the N-terminal region of the protein (Meunier et al., 2016; Schoenberger & Agarwal, 2013; Warwick, Gibson, Sood, & Lotery, 2015) (Figure 3). Segregation analysis in 60 family members showed co-segregation with disease in 47 individuals of family 1 (Figure 1a). In addition, the mutation was identified in 13 individuals who, as far as we know, do not present with a SFD phenotype yet and are indicated with a black dot on the pedigree (Figure 1a). Subsequently, the same N-terminal mutation was identified in two additional SFD families, family 2 and 3 (Figure 1b,c). The mutation segregated with disease in four individuals of family 2.

3.3 | The p.(Ser38Cys) mutation is a founder mutation

Two of the SFD families in which the p.(Ser38Cys) mutation segregates are of Belgian descent (family 1 and 3) and one is French (family 2). Haplotype reconstruction for all three families was done, as we assumed a common origin of this mutation. We genotyped 35 SNPs, covering a 9 Mb region surrounding the *TIMP3* gene, in five patients (IV:31, IV:56, IV:59, V:30, and V:33) of family 1, two patients of family 2 (II:1 and II:2), and the proband (I:1) of family 3. Interestingly, all individuals harbored the same haplotype up to a distance of 5.6 Mb upstream and 737 kb downstream of *TIMP3* (Figure 4). Overall, this showed a shared region of about 6.4 Mb, suggesting that this mutation originates from an ancient common ancestor.

3.4 | The p.(Ser38Cys) mutation does not alter *TIMP3* mRNA expression

To exclude whether the p.(Ser38Cys) mutation affects *TIMP3* mRNA expression, RT-qPCR expression analysis was performed on total RNA extracted from fibroblast samples. No difference in *TIMP3* expression levels was observed between two affected individuals of family 1 (IV:56 and IV:59) and four age-matched control individuals (unpaired *t*-test, *p*-value = 0.2) (data not shown).

3.5 | The p.(Ser38Cys) mutation does not lead to the formation of higher-molecular weight proteins

To study the effect of the identified mutation on protein level, we performed extensive Western blot analyses on whole cell lysates and ECM extracts of patient and control fibroblasts using two different lysis

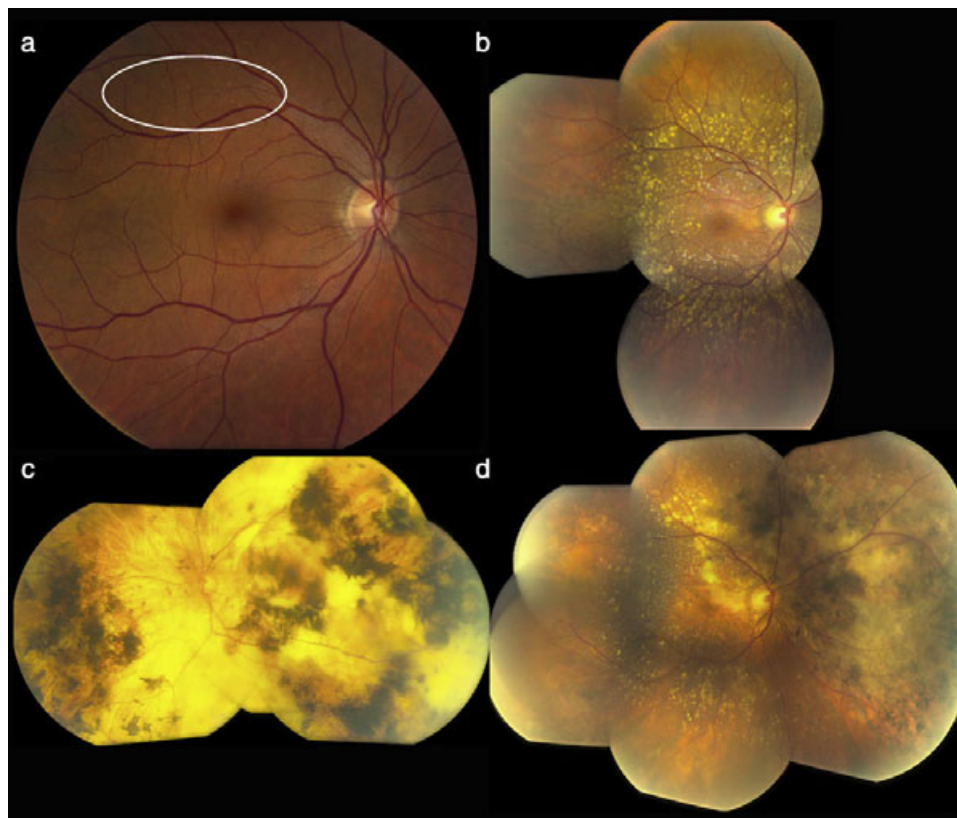


FIGURE 2 Composite of clinical images. (a) Posterior pole of right eye of a 51-year-old male patient with minimal drusen, more pronounced around the superior avascular arcades (ellipse). (b,c) Composite of posterior pole and mid-periphery of right eye of female patient at ages 65 and 72 years, respectively, illustrating evolution of phenotype over time with drusen in macula and around vascular arcades as well as patchy outer retinal atrophy (b), evolving to widespread chorioretinal atrophy, macular atrophy and subretinal neovascularization, and exudation and hyperpigmentation over a period of 7 years (c). (d) Left eye of a 74-year old female patient showing complete outer retinal atrophy, extreme hyperpigmentation, exudation consequent upon subretinal neovascularization, and fibrosis

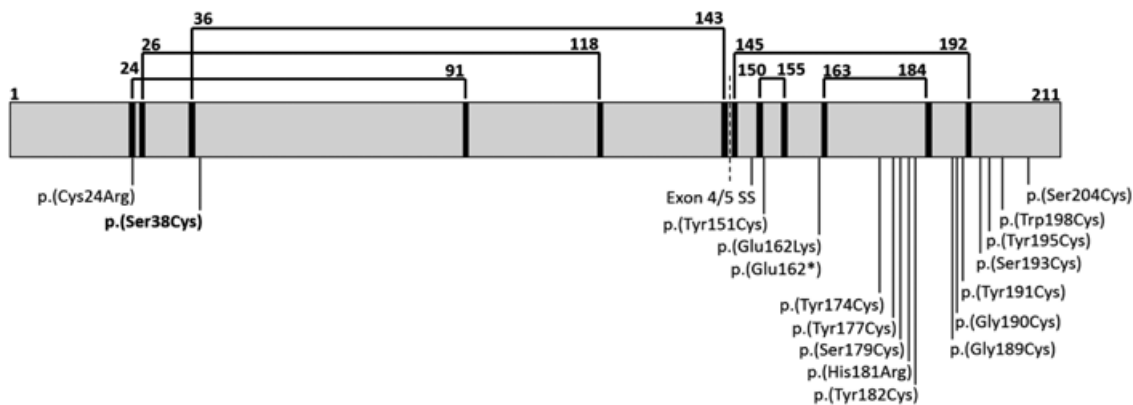


FIGURE 3 TIMP3 protein structure and SFD causing mutations. Cysteine residues are indicated with black boxes and corresponding disulfide bridges with connecting black lines (UniProtKB P35625). Known mutations are indicated beneath the figure (RefSeq NM_000362.4, NP_000353). The mutation studied here is indicated in bold. The N- and C- terminal domains are separated by a dashed line (Bakall et al., 2014; Barbazetto, Hayashi, Klais, Yannuzzi, & Allikmets, 2005; Felbor et al., 1996; Felbor, Stohr, Amann, Schonherr, & Weber, 1995; Felbor, Suvanto, Forsius, Eriksson, & Weber, 1997; Fung, Stöhr, Weber, Holz, & Yannuzzi, 2013; Gliem et al., 2015; Jacobson et al., 1995, 2002; Langton et al., 2000; Lin et al., 2006; Saihan et al., 2009; Schoenberger & Agarwal, 2013; Tabata, Isashiki, Kamimura, Nakao, & Ohba, 1998; Weber et al., 1994)

buffers, both reducing and nonreducing conditions, and three different anti-TIMP3 antibodies, each recognizing a different epitope. TIMP3 and its glycosylated form have a respective molecular weight of 25 and 27 kDa and can be seen on all blots using patient fibroblasts (Figure 5a–f). We confirmed TIMP3 localization to the ECM,

as ECM extracts show a clear enrichment in TIMP3 protein (Figure 5e,f).

Western blot analysis was performed on whole cell lysate using Laemmli lysis buffer and two different antibodies (Calbiochem, Sigma) (Figure 5a,b). Statements about higher-molecular weight forms

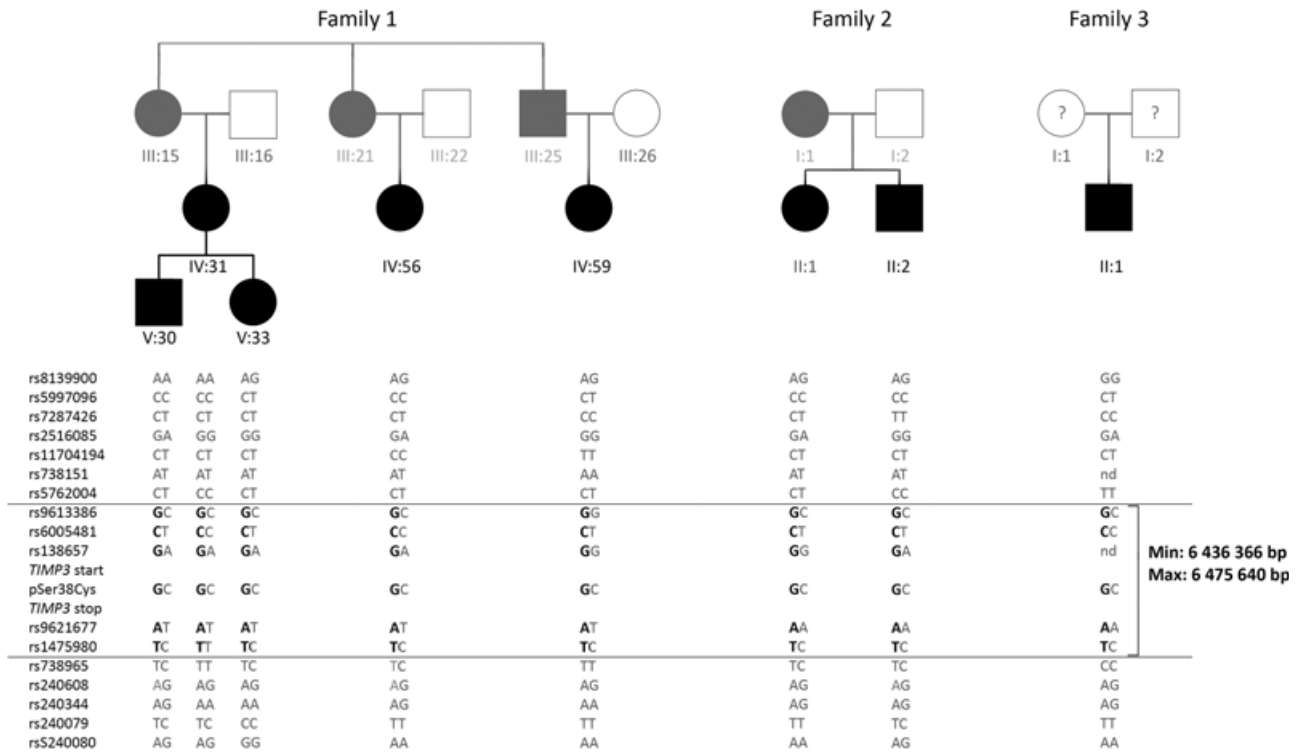


FIGURE 4 Haplotype reconstruction. SNPs covering a 9 Mb region around the *TIMP3* gene revealed a shared haplotype of maximal 6.47 Mb. Only a selection of relevant markers is shown. For full marker data, see Supporting Information Table S2

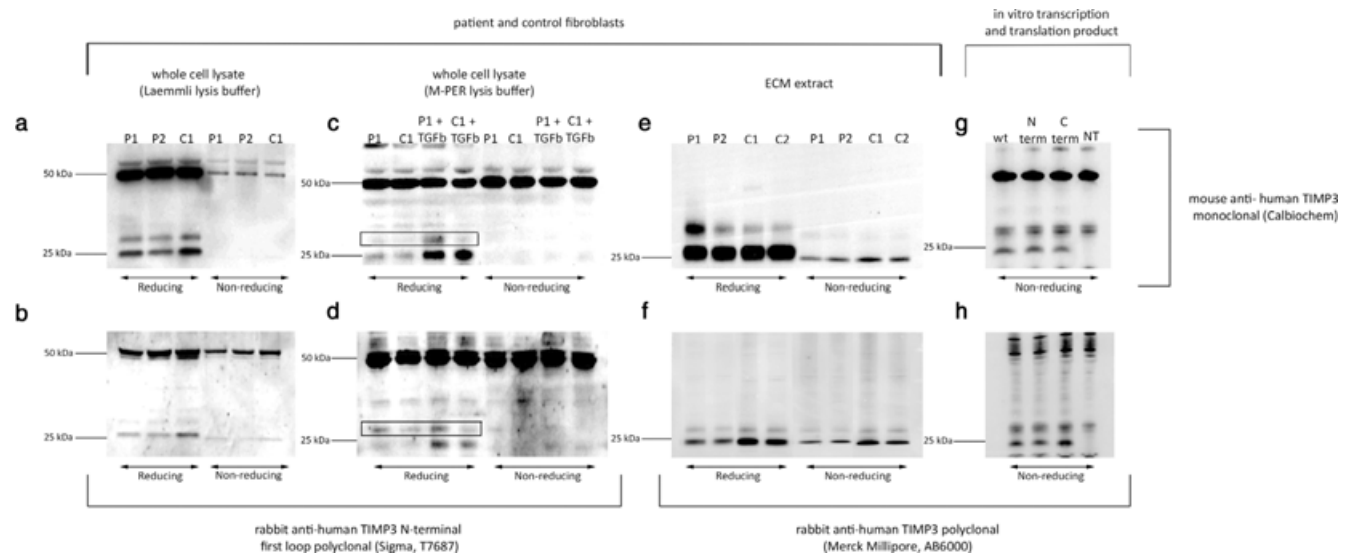


FIGURE 5 Overview of TIMP3 Western blot experiments. (a–d) Western blot analysis on whole cell lysates of patient and control fibroblasts using two lysis buffers (a,b: Laemmli; c,d: M-PER) and two primary TIMP3 antibodies (a,c: Calbiochem; b,d: Sigma). (e,f) Western blot analysis on ECM extracts of patient and control fibroblasts using two primary TIMP3 antibodies (e: Calbiochem; f: Merck). (g,h) Western blot analysis on *in vitro* transcription and translation products of wild type and mutant TIMP3 constructs using two primary TIMP3 antibodies (g: Calbiochem; h: Merck). TIMP3 and glycosylated TIMP3 have a respective molecular weight of 25 and 27 kDa. Previous hypotheses about higher-molecular weight proteins could not be confirmed, however mild hyperglycosylation was observed in patients versus controls when using M-PER lysis buffer (c,d). Abbreviations used: P = patient, C = control, ECM = extracellular matrix, TGFβ = transforming growth factor beta, wt = wild type TIMP3, N term = TIMP3 with N terminal mutation p.(Ser38Cys), C term = TIMP3 with C terminal mutation p.(Ser179Cys), NT = no template control

occurring only in patients could not be made as nonspecific bands, observed in both patients and controls, mask the region around 50 kDa where TIMP3 dimers are expected (Arris et al., 2003; Langton et al., 1998; Langton et al., 2005; Langton et al., 2000; Saihan et al., 2009; Soboleva et al., 2003; Weber et al., 2002; Yeow et al., 2002). Importantly,

this band does not disappear when samples are reduced with 1 M 1,4-dithiothreitol (DTT), which is more suggestive of nonspecific binding of both antibodies rather than TIMP3 dimerization (Figure 5a,b). As TIMP3 is known to localize to the ECM (Li et al., 2005), ECM extracts were collected of patient and control fibroblasts.

Western blot analysis on these extracts was performed, using the same antibody as in Figure 5a (Calbiochem) (Figure 5e). We cannot explain the increased intensity of glycosylated TIMP3 in P1, which was not present anymore when repeating the experiment on new ECM extracts using a third antibody (Merck) (Figure 5f). More interestingly, the nonspecific band at 50 kDa seen in Figure 5a,b was not present in the ECM extracts using two different antibodies (Calbiochem, Merck) (Figure 5e,f). This observation is an additional argument for nonspecific binding of the primary antibody to proteins present in the whole cell lysate, but not present in the ECM extracts. Furthermore, we do not observe TIMP3 dimers/multimers present in patient ECM extracts. Based on these observations, we cannot confirm the hypothesis on TIMP3 dimerization proposed by Arris et al. and others for distinct TIMP3 mutations, using the same antibody (Sigma) and fibroblast extracts (Arris et al., 2003; Weber et al., 2002).

Next, cell lysis was performed with M-PER mammalian protein extraction reagent (Thermo Fisher Scientific), which provides a milder cell lysis than Laemmli lysis buffer and keeps the proteins in their native state (Figure 5c,d). Interestingly, subsequent Western blot analysis revealed a (minor) increase in glycosylated TIMP3 in reduced patient versus control samples and this effect was even increased upon stimulation of TIMP3 expression using TGF β 1 (Su, DiBattista, Sun, Li, & Zafarullah, 1998) (Figure 5c,d). This effect was quantified on three independent Western blots using densitometry for one patient and one control sample with endogenous (-TGF β) protein expression, and relative densities of glycosylated TIMP3 to the total amount of TIMP3 were calculated. Patient samples show a statistically significant increase in glycosylation compared to control samples ($p = 0.0016$) (Supporting Information Figure S2).

Finally, we performed nonreducing Western blot analysis on WT and the following mutant TIMP3 proteins, all created by *in vitro* transcription and translation of TIMP3 expression vectors: p.(Ser38Cys) (N-terminal domain) and p.(Ser179Cys) (C-terminal domain). Again, no differences were observed between unglycosylated WT and mutated forms of TIMP3. All other bands are aspecific as they also occur in the negative control sample, where no plasmid was added to the *in vitro* transcription and translation reaction (Figure 5g,h).

Overall, based on all antibodies that were tested in this study, we prefer the AB6000 antibody (Merck Millipore) to analyze TIMP3 proteins, as this is the most sensitive for TIMP3 and shows the least nonspecific binding.

3.6 | Structural modeling of TIMP3–(pro-) MMP2 interaction

The crystal structure of the N-terminal domain of TIMP3 has been determined in complex with the TACE catalytic domain (PDB code CK1) (Wisniewska et al., 2008). We further built molecular models of the complete TIMP3, and of complete TIMP3 with MMP2 (Figure 6a) or pro-MMP2 (Figure 6b). Using this crystal structure and the complete TIMP3 homology model, we predicted the effect of the p.(Ser38Cys) mutation on protein stability using the structure-based predictors FoldX, DUET, SDM, mCSM, and MAESTRO (Guerois et al., 2002; Laimer

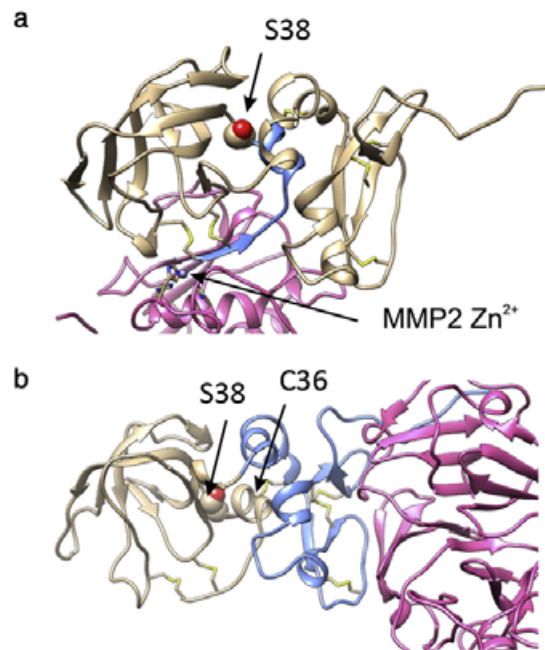


FIGURE 6 Models of TIMP3 bound to MMP2 or pro-MMP2. (a) TIMP3 is colored gray, residues 1–37 are colored blue. MMP2 is colored pink. Disulfides are displayed, and the position of Ser38 and the MMP2 active site are indicated. (b) The N-terminal domain of TIMP3 is colored gray, the C-terminal domain is colored blue. Pro-MMP2 is colored pink. Disulfides are displayed, and the position of Ser38 and Cys36 is indicated. Ser38 is not close to the interface with MMP2 or pro-MMP2, and the p.(Ser38Cys) mutation does not strongly affect stability or structure of the TIMP3 protein. Interestingly, Ser38 is close to Cys36, which forms a disulfide bridge with Cys143 in wild type TIMP3

et al., 2015; Pires et al., 2014). Prediction results did not agree well and suggested that the mutation is either moderately stabilizing, neutral, or at best moderately destabilizing, with a maximum destabilizing $\Delta\Delta G$ of $-0.84 \text{ kcal}\cdot\text{mol}^{-1}$ (Supporting Information Table S4), which is in concordance with the Western blot results showing no difference in protein expression between wild type and mutant forms of TIMP3. In the crystal structure and homology models, Ser38 is not close to the TIMP3 interface with TACE, MMP2 (Figure 6a) or pro-MMP2 (Figure 6b). However, a p.(Ser38Cys) mutation could affect the binding by long-range structural effects. We further mutated Ser38 to cysteine in the structure and homology model, followed by analyses of the mutant and WT protein using the Yasara md_refine protocol (Krieger et al., 2009). This protocol combines short molecular dynamics and energy minimization with the YASARA2 forcefield, and on average improves protein structure models (Krieger et al., 2009). This approach does not indicate any remarkable effect of the p.(Ser38Cys) mutation on the protein structure. Together, stability prediction and modeling do not provide convincing indications that a p.(Ser38Cys) mutation strongly affects stability or structure of the TIMP3 protein.

However, these approaches cannot predict the consequences of the introduction of the new cysteine on misfolding due to faulty new disulfide bridges during the folding process. For example, Ser38 is in close proximity to Cys36, which forms a disulfide bridge with Cys143

(Figure 6b). A cysteine at position 38 may compete with this correct disulfide bridge formation and interact with Cys36 to form a novel, aberrant disulfide bond.

3.7 | The p.(Ser38Cys) mutation possibly disrupts an intramolecular disulfide bond

As we hypothesize that the Cys36-Cys143 disulfide bond may be disrupted by the introduction of the p.(Ser38Cys) mutation, we performed Western blot analysis with WT and mutant p.(Ser38Cys) and p.(Ser179Cys) TIMP3 proteins generated by *in vitro* transcription and translation. Disturbance of the Cys36-Cys143 bond, covalently tethering the C-terminal and N-terminal domain, and aberrant disulfide bond formation with the cysteine at position 38, is expected to give rise to a (moderate) change in apparent molecular weight. To be able to detect small differences in molecular weight, protein gels were used with an increased separation capacity between 20 and 30 kDa. Six independent high-resolution Western blots using nonreducing conditions showed an increase in apparent molecular weight for the protein containing the N-terminal p.(Ser38Cys) mutation compared to WT TIMP3 and the C-terminal p.(Ser179Cys) mutation. Moreover, this shift in molecular weight disappears when reducing the samples with 1 M DTT, which further supports aberrant disulfide bond formation (Supporting Information Figure S3).

To confirm this hypothesis, additional TIMP3 constructs containing a p.(Cys36Ser) or p.(Cys143Ser) mutation, disrupting the wild type Cys36-Cys143 disulfide bond, were generated in combination with the WT or mutant p.(Ser38Cys) construct (Figure 7). Interestingly, we could detect a similar upward shift in apparent molecular weight on five independent nonreduced Western blots between the mutant p.(Ser38Cys) construct (Figure 7a, lane 2) and the construct containing both the p.(Ser38Cys) and p.(Cys143Ser) mutations, suggesting that the shift of the Ser38Cys mutant is not caused by a *de novo* Cys38-Cys143 disulfide bond (Figure 7a, lane 7). In contrast, the upward shift of the p.(Ser38Cys) mutation was abolished when using a plasmid that combines a p.(Ser38Cys) and p.(Cys36Ser) mutation, suggesting that the upward shift requires Cys36 (Figure 7a, lane 6). Overall these data suggest that Cys38 may indeed form an aberrant disulfide bridge with Cys36 (Figure 7c). The combination of WT TIMP3 and the mutant p.(Ser38Cys) construct (Figure 7a, lane 3), mimicking a heterozygous situation as observed in the patients, results in a broad band with a size overlapping with both the WT construct and the p.(Ser38Cys) construct, suggesting that both protein forms are represented.

4 | DISCUSSION

We have identified the causal mutation of SFD in three different families from Belgian or French origin. All affected individuals are heterozygous for the c.113C>G, p.(Ser38Cys) mutation in exon 1 of the TIMP3 gene, which was previously missed in family 1 due to less sensitive screening methods (Figure 1). This mutation has been associated with relatively late onset SFD leading to choroidal neovascularization, with or without pulmonary involvement (Meunier et al., 2016;

Schoenberger & Agarwal, 2013; Warwick et al., 2015). We confirm a later onset in the families identified here, segregating the p.(Ser38Cys) mutation. The majority of patients remained completely asymptomatic way into their fifth decade, with optimal visual function in almost all individuals until the sixth decade. Older individuals often had lost their eyesight due to complicated CNV's in the absence of treatment with anti-VEGF (Figure 2, Supporting Information Table S3). A strict follow-up, including self-monitoring, is advised to all younger patients in order to start anti-VEGF treatment at the earliest sign of CNV development. Macular atrophy is an important part of the Sorsby clinical spectrum. With the later onset of visual problems in our families compared to typical SFD, the phenotype could be mistaken for AMD. However, (mid-)peripheral changes occur at an earlier age compared to AMD and know a more rapid spread and progression. Despite the clinical heterogeneity, we found evidence of genetic homogeneity. Haplotype reconstruction of 35 genetic markers revealed a common haplotype of maximal 6.47 Mb, which points to a founder mutation originating from an ancient ancestor in the Western-European population (Figure 4).

To date, 18 different TIMP3 mutations have been identified to cause SFD (Figure 3). The mechanisms underlying TIMP3-associated SFD remain largely unidentified. The p.(Ser38Cys) mutation is one of the two located in the N-terminal region of TIMP3, which functions in MMP inhibition. As most TIMP3 mutations, p.(Ser38Cys) adds an additional cysteine to the protein, in which 12 conserved cysteines make up six disulfide bridges that are crucial for folding and structural stability of the protein. These bridges are essential for proteins destined for the secretory pathway, such as TIMP3, as they are exposed to highly oxidizing environments (Bechtel & Weerapana, 2017; Ellgaard, McCaul, Chatsisvili, & Braakman, 2016).

So far, it is unclear how the disease develops and a mechanism explaining the pathogenicity of TIMP3 mutations is currently lacking. A first hypothesis suggests a gain of function whereby mutant TIMP3 proteins containing an unpaired cysteine form abnormal disulfide-bonded dimers and aggregates that slow down turnover in the Bruch membrane (Langton et al., 2000). Dimerization/multimerization of the mutant protein has been shown for different C-terminal mutations (Arris et al., 2003; Christensen et al., 2017; Langton et al., 1998; Langton et al., 2005; Saihan et al., 2009; Soboleva et al., 2003; Weber et al., 2002; Yeow et al., 2002) (Supporting Information Table S5). However, some discrepancies remain on the ability of mutant proteins to dimerize/oligomerize, depending on the cell line or expression construct used (Langton et al., 2005). Furthermore, this hypothesis is less likely for mutations that do not lead to the gain or loss of a cysteine (Lin et al., 2006; Saihan et al., 2009). A second hypothesis involves reduced capacity of mutant TIMP3 to inhibit MMP activity or VEGF signaling. Again contradictory results exist, where a retained MMP inhibitory function was shown for the majority but not all of TIMP3 mutations evaluated (Christensen et al., 2017; Langton et al., 2005; Langton et al., 2000; Qi et al., 2002; Yeow et al., 2002) (Supporting Information Table S5).

No functional data concerning the p.(Ser38Cys) mutation are currently available. As this mutation gives rise to an unpaired cysteine, we performed extensive Western blot analyses on different sample types and using different antibodies to assess the presence of TIMP3

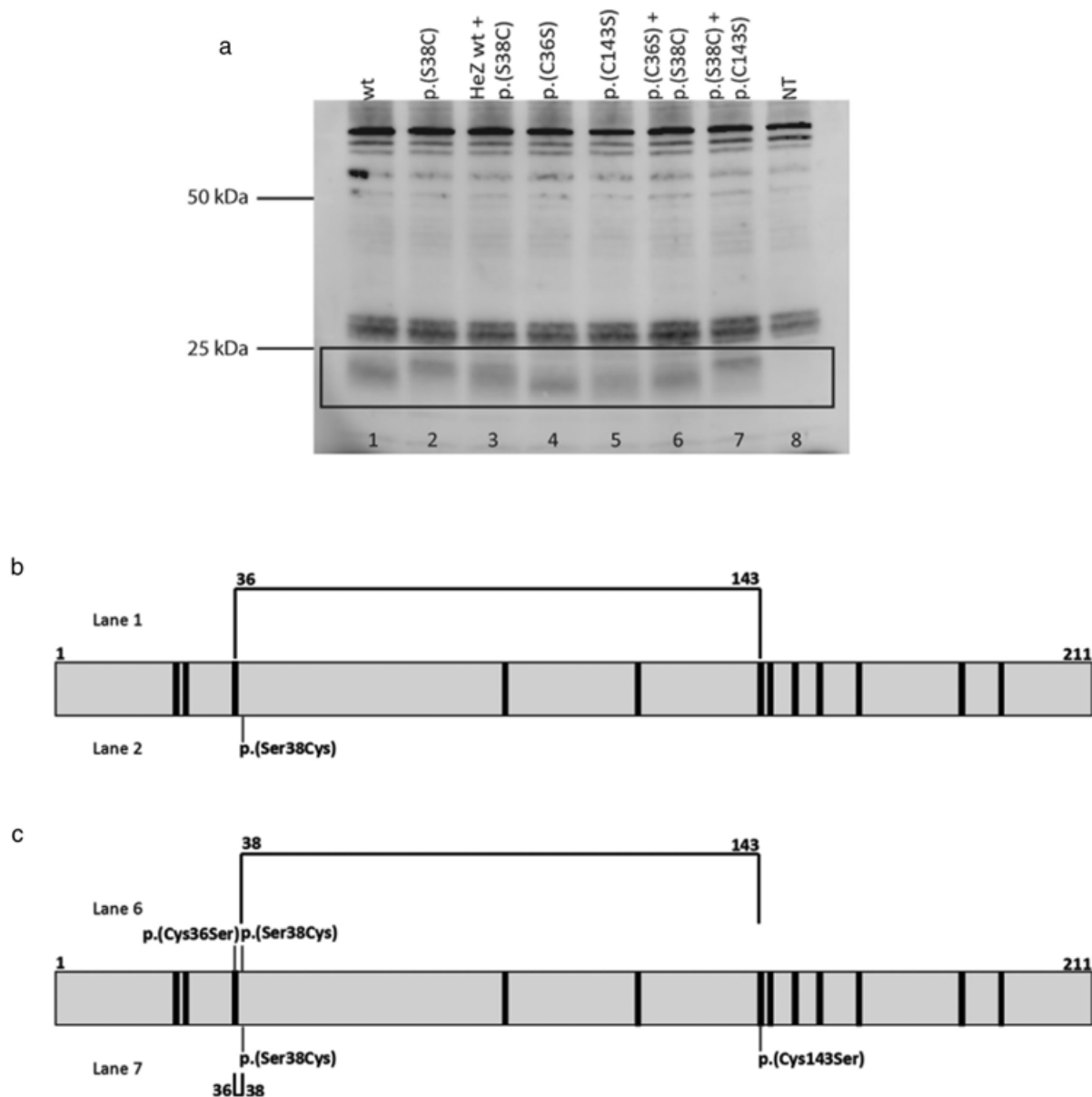


FIGURE 7 Nonreduced TIMP3 Western blot using *in vitro* transcription and translation proteins. (a) Western blot of wild type or mutant TIMP3 constructs containing (combinations of) the mutation of interest and p.(Cys36Ser) or p.(Cys143Ser), which disrupt the wild type Cys36-Cys143 disulfide bond. (b) The p.(Ser38Cys) mutation disturbs an intramolecular disulfide bond, which can be seen as an increase in molecular weight (a, lane 2). (c) Combination of the p.(Ser38Cys) and p.(Cys143Ser) mutation disturbs formation of the Cys36-Cys143 disulfide bond and induces Cys36-Cys38 disulfide bond formation (a, lane 7), which leads to the same shift in molecular weight as observed for p.(Ser38Cys) alone (a, lane 2)

dimers (Figure 5). We could, however, not identify protein aggregates in any experiment. Two antibodies (T7687, Sigma and MAB3318, Calbiochem) detected a strong immunoreactive band at 50 kDa in whole cell lysates (but not ECM), which did not disappear following 1 M DTT reduction. Furthermore, this band was also present in the no template control of an *in vitro* transcription and translation reaction, which suggests that these are nonspecific bands arising from proteins present in whole cell lysates. A third antibody (Merck) confirmed the absence of TIMP3 dimers/multimers in patient ECM extracts and *in vitro* derived mutant protein. Overall, our findings do not support TIMP3 dimerization for the p.(Ser38Cys) mutation.

Molecular modeling of the mutant TIMP3 protein together with two of its interaction partners, MMP2 and pro-MMP2, did not sug-

gest a direct effect of the p.(Ser38Cys) mutation on protein stability, or reveal a disturbance in interaction pattern as the mutation is not close to the interaction interfaces with MMP2 or pro-MMP2 (Figure 6). However, these predictions do not take into account alterations of the disulfide bridge pattern. In wild type TIMP3, Cys36 forms a disulfide bond with Cys143, covalently tethering the N-terminal and C-terminal domain of the protein. As p.(Ser38Cys) is in close proximity to Cys36 (Figure 6), we hypothesized a disruption of the Cys36-Cys143 disulfide bond and potential formation of a novel one. This hypothesis was subsequently confirmed by high-resolution Western blot analysis of p.(Ser38Cys) mutant protein compared to wild type or p.(Ser179Cys) mutant protein (Supporting Information Figure S3), showing an upward shift in apparent molecular weight of the

p.(Ser38Cys) mutant TIMP3 compared to wild type or p.(Ser179Cys) mutant protein. The shift disappears when reducing the samples with 1 M DTT, which disrupt disulfide bonds, thus confirming that the identified shift indeed arose from abnormal disulfide bonding. Further experiments with combined mutants of the Cys36, Ser38, and Cys143 residues suggested formation of a *de novo* Cys36-Cys38 disulfide bridge (Figure 7). Several instances of disulfide bridged Cys-X-Cys motifs are present in the PDB structure database. Importantly, this change in intramolecular rather than intermolecular disulfide bonding due to a free cysteine might explain the absence of TIMP3 protein dimers for the p.(Ser38Cys) mutation.

The aberrant, novel Cys36-Cys38 disulfide bond is expected to affect the tertiary structure of both the N- and C-terminal domains. The disruption of the Cys36-Cys143 disulfide bridge makes the N- and C-terminal domain of the protein less tethered, which may even mean that the p.(Ser38Cys) mutation in the N-terminal domain *de facto* affects the function of the C-terminal domain. This is interesting, as it is striking that the vast majority of TIMP3 mutations in SFD occur in the C-terminal domain (Figure 3). The C-terminal domain ascertains the interaction with the ECM, inhibits activation of pro-MMPs and binding of VEGF to VEGFR2 (Brew & Nagase, 2010; Nagase et al., 2006; Qi & Anand-Apte, 2015), and interacts with EFEMP1 (Klenotic, Munier, Marmorstein, & Anand-Apte, 2004).

Interestingly, the TIMP3 C-terminal domain contains a single N-glycosylation site at Asn207, which is part of the pro-MMP2 binding site. For other TIMPs, it has already been suggested that an early, intracellular interaction between TIMPs and pro-MMPs can affect protein maturation such as glycosylation (Roderfeld et al., 2007). It is therefore possible that the faulty disulfide bonding alters the binding affinity of TIMP3 to its C-terminal binding partners such as pro-MMPs, which could influence glycosylation of the TIMP3 protein. In this respect, we detected a moderate increase in TIMP3 glycosylation in whole cell lysate from one patient compared to a control (Figure 5c,d). However, obtaining access to additional patient samples would be of interest to further support this finding.

This observation is reminiscent to the findings of Qi et al., who identified a similar difference in glycosylation status for the SFD p.(Ser179Cys) C-terminal mutation. Possible consequences of excessive glycosylation are reduced binding to the ECM by masking basic residues in the protein and a reduced MMP inhibitory function due to a conformational change (Qi et al., 2009).

Importantly, the exact effect of the altered intramolecular bonding caused by p.(Ser38Cys) on the glycosylation status and function of TIMP3, such as binding/inhibition of (pro-) MMPs, VEGFR2, or EFEMP1, is currently unknown. Both gain of function and loss of function are possible. In a gain of function model, the aberrantly folded mutant protein is less prone to degradation than the wild type protein and leads to accumulation of TIMP3 in the Bruch membrane. Eventually this would lead to disruption of the RPE, as seen in SFD patients. In a loss of function model, the mutant protein has a reduced ability to inhibit MMPs or VEGF, which would lead to ECM dysregulation and CNV (Christensen et al., 2017). Further research is necessary to determine which model is applicable for the p.(Ser38Cys) mutation and if all SFD-variants have a shared disease mechanism.

In the current study patient-derived fibroblasts were used, similar to previous papers (Arris et al., 2003; Weber et al., 2002). However, given the major involvement of the RPE, other cell types such as induced pluripotent stem cell (iPSC)—derived RPE from patients with SFD would be of interest in assessing the downstream effect of the altered intramolecular disulfide bonding and how this mutation affects the RPE. This cell type already showed great potency in mimicking adult human RPE and it has been shown that iPSC-RPE from patients with SFD exhibits drusen and ECM alterations (Galloway et al., 2017).

In conclusion, we identified a heterozygous *TIMP3* founder mutation (c.113C>G, p.(Ser38Cys)) in three families with late-onset SFD. We were not able to confirm the general hypothesis on abnormal intermolecular disulfide bonding resulting in aberrant TIMP3 protein dimerization. Instead, we propose a novel pathogenetic mechanism for this N-terminal mutation comprising the formation of a novel intramolecular disulfide bond with a potential effect on TIMP3 glycosylation.


ACKNOWLEDGMENTS

This work was supported by the Institute for Innovation by Science and Technology (IWT), integrated in the FWO (FWO-SB) (S.N.). D.S. is a postdoctoral fellow of the FWO. B.P.L. is Senior Clinical Investigator of the FWO. We gratefully acknowledge the families who participated in this study and thank Sarah De Jaegere and Brecht Guillemyn for their assistance with experiments and Nico Callewaert for sharing his insights into glycosylation of TIMPs.

CONFLICTS OF INTEREST

F.C. is a co-founder of pxlence.

ORCID

Sarah Naessens  <https://orcid.org/0000-0001-9080-3103>

Julie De Zaeytijd  <https://orcid.org/0000-0003-4035-6389>

Delfien Syx  <https://orcid.org/0000-0001-9421-4496>

Roosmarijn E. Vandenbroucke 


<https://orcid.org/0000-0002-8327-620X>

Frédéric Smeets  <https://orcid.org/0000-0002-7191-1456>

Caroline Van Cauwenbergh 

<https://orcid.org/0000-0002-1948-9091>

Bart P. Leroy  <https://orcid.org/0000-0002-9899-2081>

Frank Peelman  <https://orcid.org/0000-0001-6852-8731>

Frauke Coppieters  <https://orcid.org/0000-0001-7224-0992>

REFERENCES

- Arris, C. E., Bevitt, D. J., Mohamed, J., Li, Z., Langton, K. P., Barker, M. D., ... McKie, N. (2003). Expression of mutant and wild-type TIMP3 in primary gingival fibroblasts from Sorsby's fundus dystrophy patients. *Biochimica et Biophysica Acta (BBA)—Molecular Basis of Disease*, 1638(1), 20–28. Retrieved from [http://doi.org/10.1016/S0925-4439\(03\)00036-X](http://doi.org/10.1016/S0925-4439(03)00036-X)
- Assink, J. J. M., De Backer, E., Brink, J. B., Kohno, T., De Jong, P. T. V. M., Bergen, A. A. B., & Meire, F. (2000). Sorsby fundus dystrophy without a mutation in the TIMP-3 gene. *British Journal of Ophthalmology*, 84, 682–686.

- Bakall, B., Sohn, E. H., Riley, J., Brack, D., & Stone, E. M. (2014). Novel mutations and change of nomenclature for pathogenic variants in the TIMP3 gene causing Sorsby fundus dystrophy. *Investigative Ophthalmology & Visual Science*, 55(13), 3290.
- Barbazetto, I. A., Hayashi, M., Klais, C. M., Yannuzzi, L. A., & Allikmets, R. (2005). A novel TIMP3 mutation associated with Sorsby fundus dystrophy. *Archives of Ophthalmology*, 123, 542–543.
- Bechtel, T. J., & Weerapana, E. (2017). From structure to redox: The diverse functional roles of disulfides and implications in disease. *Proteomics*, 17(6), 1–34. Retrieved from <http://doi.org/10.1002/pmic.201600391>
- Brew, K., & Nagase, H. (2010). The tissue inhibitors of metalloproteinases (TIMPs): An ancient family with structural and functional diversity. *Biochimica et Biophysica Acta*, 1803(1), 55–71. Retrieved from <http://doi.org/10.1007/s11103-011-9767-z>.Plastid
- Christensen, D. R. G., Brown, F. E., Cree, A. J., Ratnayaka, J. A., & Lotery, A. J. (2017). Sorsby fundus dystrophy—A review of pathology and disease mechanisms. *Experimental Eye Research*, 165, 35–46. Retrieved from <http://doi.org/10.1016/j.exer.2017.08.014>
- Clark, I. M., Swingler, T. E., Sampieri, C. L., & Edwards, D. R. (2008). The regulation of matrix metalloproteinases and their inhibitors. *The International Journal of Biochemistry & Cell Biology*, 40, 1362–1378. Retrieved from <http://doi.org/10.1016/j.biocel.2007.12.006>
- Ellgaard, L., McCaul, N., Chatsivivili, A., & Braakman, I. (2016). Co- and post-translational protein folding in the ER. *Traffic*, 17, 615–638. Retrieved from <http://doi.org/10.1111/tra.12392>
- Felbor, U., Benkwitz, C., Klein, M. L., Greenberg, J., Gregory, C. Y., & Weber, B. H. F. (1997). Sorsby fundus dystrophy: Reevaluation of variable expressivity in patients carrying a TIMP3 founder mutation. *Archives of Ophthalmology*, 115, 1569–1571.
- Felbor, U., Stohr, H., Amann, T., Schonherr, U., Apfelstedt-sylla, E., Weber, B. H. F., & Felbor, U. (1996). A second independent Tyr168Cys mutation in the tissue inhibitor of metalloproteinases-3 (TIMP3) in Sorsby's fundus dystrophy. *Journal of Medical Genetics*, 33, 233–236.
- Felbor, U., Stohr, H., Amann, T., Schonherr, U., & Weber, B. H. F. (1995). A novel Ser156Cys mutation in the tissue inhibitor of metalloproteinases-3 (TIMP3) in Sorsby's fundus dystrophy with unusual clinical features. *Human Molecular Genetics*, 4, 2415–2416.
- Felbor, U., Suvanto, E. A., Forsius, H. R., Eriksson, A. W., & Weber, B. H. F. (1997). Autosomal recessive Sorsby fundus dystrophy revisited: Molecular evidence for dominant inheritance. *American Journal of Human Genetics*, 60, 57–62.
- Fung, A. T., Stöhr, H., Weber, B. H. F., Holz, F. G., & Yannuzzi, L. A. (2013). Atypical Sorsby fundus dystrophy with a novel tyr159cys timp-3 mutation. *Retinal Cases and Brief Reports*, 7(1), 71–74. Retrieved from <http://doi.org/10.1097/ICB.0b013e318267101e>
- Galloway, C. A., Dalvi, S., Hung, S. S. C., MacDonald, L. A., Latchney, L. R., Wong, R. C. B., ... Singh, R. (2017). Drusen in patient-derived hiPSC-RPE models of macular dystrophies. *Proceedings of the National Academy of Sciences*, 10, 430. Retrieved from <http://doi.org/10.1073/pnas.1710430114>
- Gliem, M., Müller, P. L., Mangold, E., Holz, F. G., Bolz, H. J., Stöhr, H., ... Issa, C. (2015). Sorsby fundus dystrophy: Novel mutations, novel phenotypic characteristics, and treatment outcomes. *Investigative Ophthalmology & Visual Science*, 56(4), 2664. Retrieved from <http://doi.org/10.1167/iovs.14-15733>
- Gourier, H., & Chong, V. (2015). Can novel treatment of age-related macular degeneration be developed by better understanding of Sorsby's fundus dystrophy. *Journal of Clinical Medicine*, 4, 874–883. Retrieved from <http://doi.org/10.3390/jcm4050874>
- Guerois, R., Nielsen, J. E., & Serrano, L. (2002). Predicting changes in the stability of proteins and protein complexes: A study of more than 1000 mutations. *Journal of Molecular Biology*, 320, 369–387. Retrieved from [http://doi.org/10.1016/S0022-2836\(02\)00442-4](http://doi.org/10.1016/S0022-2836(02)00442-4)
- Jacobson, S. G., Cideciyan, A. V., Bennett, J., Kingsley, R. M., Sheffield, V. C., & Stone, E. M. (2002). Novel mutation in the TIMP3 gene causes Sorsby fundus dystrophy. *Archives of Ophthalmology*, 120, 376–379.
- Jacobson, S. G., Cideciyan, A. V., Regunath, G., Rodriguez, F. J., Vandenburgh, K., Sheffield, V. C., & Stone, E. M. (1995). Night blindness in Sorsby's fundus dystrophy reversed by vitamin A. *Nature Genetics*, 11, 27–32.
- Kamei, M., & Hollyfield, J. G. (1999). TIMP-3 in Bruch's membrane: Changes during aging and in age-related macular degeneration. *Investigative Ophthalmology & Visual Science*, 40(10), 2367–2375.
- Katoh, K., & Standley, D. M. (2013). MAFFT multiple sequence alignment software version 7: Improvements in performance and usability. *Molecular Biology and Evolution*, 30, 772–780. Retrieved from <http://doi.org/10.1093/molbev/mst010>
- Klenotic, P. A., Munier, F. L., Marmorstein, L. Y., & Anand-Apte, B. (2004). Tissue inhibitor of metalloproteinases-3 (TIMP-3) is a binding partner of epithelial growth factor-containing Fibulin-like extracellular matrix protein 1 (EFEMP1). *The Journal of Biological Chemistry*, 279(29), 30469–30473. Retrieved from <http://doi.org/10.1074/jbc.M403026200>
- Krieger, E., Joo, K., Lee, J., Lee, J., Raman, S., Thompson, J., ... Karplus, K. (2009). Improving physical realism, stereochemistry and side-chain accuracy in homology modeling: Four approaches that performed well in CASP8. *Proteins*, 77(Suppl 9), 114–122. Retrieved from <http://doi.org/10.1002/prot.22570>
- Laimer, J., Hofer, H., Fritz, M., Wegenkittl, S., & Lackner, P. (2015). MAESTRO—multi agent stability prediction upon point mutations. *BMC Bioinformatics*, 16, 116. Retrieved from <http://doi.org/10.1186/s12859-015-0548-6>
- Langton, K. P., Barker, M. D., & McKie, N. (1998). Localization of the functional domains of human tissue inhibitor of metalloproteinases-3 and the effects of a Sorsby's fundus dystrophy mutation. *Journal of Biological Chemistry*, 273, 16778–16781.
- Langton, K. P., McKie, N., Curtis, A., Goodship, J. A., Bond, P. M., Barker, M. D., & Clarke, M. (2000). A novel TIMP-3 mutation reveals a common molecular phenotype in Sorsby's fundus dystrophy. *Journal of Biological Chemistry*, 275, 27027–27031. Retrieved from <http://doi.org/10.1074/jbc.M909677199>
- Langton, K. P., McKie, N., Smith, B. M., Brown, N. J., & Barker, M. D. (2005). Sorsby's fundus dystrophy mutations impair turnover of TIMP-3 by retinal pigment epithelial cells. *Human Molecular Genetics*, 14, 3579–3586. Retrieved from <http://doi.org/10.1093/hmg/ddi385>
- Lefever, S., Pattyn, F., De Wilde, B., Coppieters, F., De Keulenaer, S., Hellemans, J., & Vandesompele, J. (2017). High-throughput PCR assay design for targeted resequencing using primerXL. *BMC Bioinformatics*, 18, 1–9. Retrieved from <http://doi.org/10.1186/s12859-017-1809-3>
- Li, Z., Clarke, M. P., Barker, M. D., & McKie, N. (2005). TIMP3 mutation in Sorsby's fundus dystrophy: Molecular insights. *Expert Reviews in Molecular Medicine*, 7(24), 1–15. Retrieved from <http://doi.org/10.1017/S1462399405010045>
- Lin, R. J., Blumenkranz, M. S., Binkley, J., Wu, K., & Vollrath, D. (2006). A novel His158Arg mutation in TIMP3 causes a late-onset form of Sorsby fundus dystrophy. *American Journal of Ophthalmology*, 142, 839–848. Retrieved from <http://doi.org/10.1016/j.ajo.2006.06.003>
- Meunier, I., Bocquet, B., Labesse, G., Zeitz, C., Defoort-Dhellemmes, S., Lacroux, A., ... Hamel, C. P. (2016). A new autosomal dominant eye and lung syndrome linked to mutations in TIMP3 gene. *Scientific Reports*, 6, 32544. Retrieved from <http://doi.org/10.1038/srep32544>
- Nagase, H., Visse, R., & Murphy, G. (2006). Structure and function of matrix metalloproteinases and TIMPs. *Cardiovascular Research*, 69, 562–573. Retrieved from <http://doi.org/10.1016/j.cardiores.2005.12.002>

- Pettersen, E. F., Goddard, T. D., Huang, C. C., Couch, G. S., Greenblatt, D. M., Meng, E. C., & Ferrin, T. E. (2004). UCSF Chimera—A visualization system for exploratory research and analysis. *Journal of Computational Chemistry*, 25, 1605–1612. Retrieved from <http://doi.org/10.1002/jcc.20084>
- Pires, D. E. V., Ascher, D. B., & Blundell, T. L. (2014). DUET: A server for predicting effects of mutations on protein stability using an integrated computational approach. *Nucleic Acids Research*, 42, 314–319. Retrieved from <http://doi.org/10.1093/nar/gku411>
- Qi, J. H., & Anand-Apte, B. (2015). Tissue inhibitor of metalloproteinase-3 (TIMP3) promotes endothelial apoptosis via a caspase-independent mechanism. *Apoptosis*, 20, 523–534. Retrieved from <http://doi.org/10.1007/s10495-014-1076-y>
- Qi, J. H., Dai, G., Luthert, P., Chaurasia, S., Hollyfield, J., Weber, B. H. F., ... Anand-Apte, B. (2009). S156C mutation in tissue inhibitor of metalloproteinases-3 induces increased angiogenesis. *The Journal of Biological Chemistry*, 284, 19927–19936. Retrieved from <http://doi.org/10.1074/jbc.M109.013763>
- Qi, J. H., Ebrahem, Q., Yeow, K., Edwards, D. R., Fox, P. L., & Anand-Apte, B. (2002). Expression of Sorsby's fundus dystrophy mutations in human retinal pigment epithelial cells reduces matrix metalloproteinase inhibition and may promote angiogenesis. *The Journal of Biological Chemistry*, 277, 13394–13400. Retrieved from <http://doi.org/10.1074/jbc.M110870200>
- Roderfeld, M., Graf, J., Giese, B., Salguero-Palacios, R., Tschuschner, A., Müller-Newen, G., & Roeb, E. (2007). Latent MMP-9 is bound to TIMP-1 before secretion. *Biological Chemistry*, 388, 1227–1234. Retrieved from <http://doi.org/10.1515/BC.2007.123>
- Saihan, Z., Li, Z., Rice, J., Rana, N. A., Ramsden, S., Schlottmann, P. G., ... Webster, A. R. (2009). Clinical and biochemical effects of the E139K missense mutation in the TIMP3 gene, associated with Sorsby fundus dystrophy. *Molecular Vision*, 15, 1218–1230.
- Schoenberger, S. D., & Agarwal, A. (2013). A novel mutation at the N-terminal domain of the TIMP3 gene in Sorsby fundus dystrophy. *Retina*, 33, 429–435.
- Soboleva, G., Geis, B., Schrewe, H., & Weber, B. H. F. (2003). Sorsby fundus dystrophy mutation Timp3(S156C) affects the morphological and biochemical phenotype but not metalloproteinase homeostasis. *Journal of Cellular Physiology*, 197, 149–156. Retrieved from <http://doi.org/10.1002/jcp.10361>
- Sorsby, A., Joll Mason, M. E., & Gardener, N. (1949). A fundus dystrophy with unusual features. *The British Journal of Ophthalmology*, 33, 67–97.
- Su, S., DiBattista, J., Sun, Y., Li, W., & Zafarullah, M. (1998). Up-regulation of tissue inhibitor of metalloproteinases-3 gene expression by TGF-beta in articular chondrocytes is mediated by serine/threonine and tyrosine kinases. *Journal of Cellular Biochemistry*, 70, 517–527.
- Tabata, Y., Isashiki, Y., Kamimura, K., Nakao, K., & Ohba, N. (1998). A novel splice site mutation in the tissue inhibitor of the metalloproteinases-3 gene in Sorsby's fundus dystrophy with unusual clinical features. *Human Genetics*, 103, 179–182.
- Visse, R., & Nagase, H. (2003). Matrix metalloproteinases and tissue inhibitors of metalloproteinases: Structure, function, and biochemistry. *Circulation Research*, 92, 827–839. Retrieved from <http://doi.org/10.1161/01.RES.0000070112.80711.3D>
- Warwick, A., Gibson, J., Sood, R., & Lotery, A. (2015). A rare penetrant TIMP3 mutation confers relatively late onset choroidal neovascularisation which can mimic age-related macular degeneration. *Eye*, 30, 488–491. Retrieved from <http://doi.org/10.1038/eye.2015.204>
- Weber, B. H. F., Lin, B., White, K., Kohler, K., Soboleva, G., Herterich, S., ... Schrewe, H. (2002). A mouse model for Sorsby fundus dystrophy. *Investigative Ophthalmology & Visual Science*, 43, 2732–2740.
- Weber, B. H. F., Vogt, G., Pruett, R. C., Stöhr, H., & Felbor, U. (1994). Mutations in the tissue inhibitor of metalloproteinases-3 (TIMP3) in patients with Sorsby's fundus dystrophy. *Nature Genetics*, 8, 352–356.
- Wisniewska, M., Goettig, P., Maskos, K., Belouski, E., Winters, D., Hecht, R., ... Bode, W. (2008). Structural determinants of the ADAM inhibition by TIMP-3: Crystal structure of the TACE-N-TIMP-3 complex. *Journal of Molecular Biology*, 381, 1307–1319. Retrieved from <http://doi.org/10.1016/j.jmb.2008.06.088>
- Yeow, K. M., Kishnani, N. S., Hutton, M., Hawkes, S. P., Murphy, G., & Edwards, D. R. (2002). Sorsby's fundus dystrophy tissue inhibitor of metalloproteinases-3 (TIMP-3) mutants have unimpaired matrix metalloproteinase inhibitory activities, but affect cell adhesion to the extracellular matrix. *Matrix Biology: Journal of the International Society for Matrix Biology*, 21, 75–88. Retrieved from <http://doi.org/S0945053X01001809>

SUPPORTING INFORMATION

Additional supporting information may be found online in the Supporting Information section at the end of the article.

How to cite this article: Naessens S, De Zaeytjij J, Syx D, et al. The N-terminal p.(Ser38Cys) *TIMP3* mutation underlying Sorsby fundus dystrophy is a founder mutation disrupting an intramolecular disulfide bond. *Human Mutation*. 2019;40:539–551. <https://doi.org/10.1002/humu.23713>